Engineering Spatial Control of Bacterial Organelles

Y Hoang[1†], Pankaj. V. Jadhav [2†], Daniel S. Trettel[3], Rachel E. Dow[1], Seokmu Kwon[4], Kate Matej[5], Jordan A. Byrne[1], Christopher A. Azaldegui[1], Tobias W. Giessen[4], Hualiang Pi[5], Shyamal Mosalaganti[2,4,6,7*], and Anthony G. Vecchiarelli[1*]

[1] Department of Molecular, Cellular, and Developmental Biology, University of Michigan; Ann Arbor, MI 48109, USA

[2] Life Sciences Institute, University of Michigan; Ann Arbor, MI 48108, USA

[3] Los Alamos National Laboratory, Bioscience Division, Microbial and Biome Sciences Group; Los Alamos, NM 87544, USA

[4] Department of Biological Chemistry, University of Michigan; Ann Arbor, MI 48109, USA

[5] Department of Microbial Pathogenesis and Microbial Sciences Institute, Yale University School of Medicine; New Haven, CT 06510, USA

[6] Department of Cell and Developmental Biology, University of Michigan; Ann Arbor, MI 48109, USA

[7] Department of Biophysics, College of Literature, Science, and the Arts, University of Michigan; Ann Arbor, MI 48109, USA

[†] These authors contributed equally

* Correspondence: ave@umich.edu (A.G.V.), mosalaga@umich.edu (S.M.)

Abstract

Bacteria were once thought to lack organelles, but it is now clear they confine cellular reactions using an array of membrane- and protein-based compartments. A central question, however, is how bacterial organelles are organized in the cell, and whether their spatial control can be engineered. Here, we show that a two-protein system (McdAB) that positions carboxysomes-CO_2-fixing organelles found in autotrophic bacteria-can be repurposed to provide programmable spatial control to diverse organelles in *Escherichia coli*. McdAB not only restores proper assembly and positioning of heterologously expressed carboxysomes in *E. coli*, but can also be reprogrammed to spatially organize all other known types of bacterial organelles, including encapsulins, biomolecular condensates, and even membrane-bound organelles. Programmable spatial organization of bacterial organelles establishes a new design principle for synthetic biology, where the location of reactions is as tunable as their content. Our work paves the way for more efficient biocatalysis in engineered microbes.

Cells achieve remarkable control over biochemistry by organizing reactions in space. In bacteria, protein-based microcompartments, encapsulins, and biomolecular condensates, as well as membrane-bound organelles, enable reactions to be concentrated and regulated without the extensive endomembrane systems of eukaryotes. These self-assembling compartments have drawn broad interest as modular building blocks for synthetic biology. Yet, a central challenge limits their utility: when expressed in heterologous hosts such as *Escherichia coli*, the nucleoid acts as a diffusion barrier (*1*–*4*). As a result, without spatial control, these organelles form nucleoid-excluded aggregates at the cell pole. This asymmetric distribution in the cell results in a loss of faithful inheritance across the cell population, compromising activity and constraining their applications.

To solve this problem, most bacteria encode minimal, self-organizing systems comprised of a positioning ATPase from the partition protein A (ParA) family, along with a partner protein that links the ATPase to its cellular cargo (*5*). Unlike the linear motors and cytoskeletal systems used by eukaryotes, these two-protein positioning modules generate dynamic ATP-driven protein gradients on the nucleoid to spatially distribute a diversity of cellular cargos, including chromosomes, plasmids, protein complexes, and organelles – ensuring their faithful inheritance and robust functions in the cell. This conserved evolutionary strategy across diverse bacteria and cargo types provides a blueprint for engineering a generalizable method for programming spatial control in bacteria.

The most extensively studied bacterial organelle is the carboxysome, a protein-based organelle found in autotrophic bacteria that is responsible for roughly a third of global CO_2-fixation and holds significant promise for biotechnological applications. Carboxysome organization within the cell is mediated by the Maintenance of Carboxysome Distribution (Mcd) system (*6*, *7*). Specifically, McdB binds carboxysomes and induces McdA oscillations along the nucleoid that distribute carboxysomes throughout the cell to ensure faithful inheritance and CO_2-fixation capacity across the cell population. Without McdAB, carboxysomes mislocalize to the cell poles as nucleoid-excluded aggregates, leading to asymmetric inheritance and a rapid loss of both carboxysomes and CO_2-fixation capacity in the population (*6*, *8*, *9*).

The McdAB system is currently the only known minimal and self-organizing positioning system for any protein-based organelle in bacteria. Inspired by its natural anti-aggregation mechanism, we asked whether McdAB could be repurposed to provide synthetic spatial control. Here, we demonstrate that McdAB not only restores proper assembly and positioning of heterologously-expressed carboxysomes in *E. coli*, but also generalizes to diverse organelles, including protein-based encapsulins and condensates, as well as membrane-bound organelles. Through live-cell imaging, super-resolution microscopy, and *in situ* cryo-electron tomography, we show that McdAB

transforms disordered and mispositioned aggregates into evenly distributed, dynamic arrays. By enabling modular and reversible spatial organization, McdAB provides a versatile strategy for engineering the "*where*" of cellular reactions in bacteria and establishes spatial control as a new design axis for microbial synthetic biology and biotechnology.

Results

The McdAB system spatially organizes carboxysomes in E. coli

Carboxysomes are highly efficient CO_2-fixing organelles, and reconstituting them in *E. coli* could transform this industrial microbe into a powerful chassis for sustainable bioproduction. Yet, despite repeated attempts, engineered carboxysomes in *E. coli* remain dysfunctional. Without their native McdAB positioning system, carboxysomes mislocalize to the cell poles and exhibit poor CO_2-fixation activity (*1*, *4*, *10*, *11*). We have previously shown that even in the native autotrophic host, carboxysome mispositioning in the absence of McdAB disrupts cell growth and division (*9*). These findings underscore the importance of spatial organization for carboxysome function. Motivated by this, we set out to reconstitute not only carboxysome assembly but also its distribution system in *E. coli*.

We used the recently developed inducible 'pXpressome' plasmid toolkit to express α-carboxysomes from the chemoautotroph *Halothiobacillus neapolitanus* in *E. coli*. The small subunit of the carbon-fixing Rubisco enzyme (CbbS) was fused to monomeric NeonGreen (mNG) for *in vivo* fluorescence imaging (Fig. 1A) (*4*). As shown by others, large nucleoid-excluded foci were observed at one or both cell poles (Fig. 1A, C, D; Supplementary Fig. 1A-B). But upon co-expression of the McdAB system, carboxysomes were no longer aggregated at the cell poles (Fig. 1B-D; Supplementary Fig. 1A-B). Instead, multiple foci were distributed across the nucleoid region of the cell. Similar results were obtained when Rubisco was fused to mScarlet or mJuniper, confirming that McdAB-mediated carboxysome positioning is independent of the fluorescent tag used (Supplementary Fig. 1C-D).

Having established that McdAB restores carboxysome organization in *E. coli*, we next examined how this positioning system dynamically regulates organelle distribution in growing and dividing *E. coli* cells over time. Cells were classified based on the number and location of foci: "mispositioned" (0–2 polar foci) and "positioned" (≥3 distributed foci). Without McdAB, carboxysome foci remained mispositioned through cell growth and multiple cell divisions (Fig. 1E-F; Supplementary Fig. 1E; Video S1). In contrast, the vast majority of McdAB-expressing cells maintained distributed carboxysome foci (Fig. 1G-H; Supplementary Fig. 1F; Video S1). These results demonstrate that the McdAB system prevents polar aggregation and promotes the even distribution and increased number of α-carboxysome assemblies in *E. coli*.

While fluorescence imaging revealed that McdAB redistributes Rubisco foci across the cell, this approach lacks the necessary spatial resolution to determine whether the observed foci represent correctly assembled carboxysomes. To directly assess the ultrastructure of these assemblies in the bacterial cell, we performed *in situ* cryo-electron tomography (cryo-ET). Without McdAB, we observed large, disorganized, and tightly packed arrays of carboxysome components at the cell poles within the tomograms (Fig. 1I, Video S2). We also observed that some fully assembled carboxysomes had individual diameters ranging from 80 to 500 nm - the diameter of α-carboxysomes in *H. neapolitanus*, the native host, ranges from 80 to 120 nm (*12*). By contrast, and consistent with the fluorescence data, McdAB-expressing cells displayed fully assembled, properly sized, and unclustered carboxysomes distributed across the nucleoid region of the cell volume (Fig. 1J, Video S2). Strikingly, we also observed in our *in situ* cryo-tomograms carboxysome "partitioning," where the shell appears to invaginate at the midpoint of a larger carboxysome (Supplementary Fig. 1G, white arrowheads), suggesting that McdAB may play a role in carboxysome assembly and size regulation by subdividing oversized structures.

Taken together, these findings provide direct evidence that McdAB is a truly minimal and self-organizing positioning system - requiring only two proteins to distribute carboxysomes in a heterologous host - while simultaneously promoting their structural integrity and proper assembly.

Spatial control of encapsulin nanocompartments

Building on our discovery that McdAB is minimal and self-organizing, we aimed to repurpose it as a versatile spatial regulator for other bacterial organelles. We recently identified an N-terminal peptide of McdB that is necessary and sufficient for McdA interaction (*13*). Here, we sought to develop this McdB peptide into a minimal autonomous positioning tag or "MapTag". By fusing this MapTag to heterologous organelles and co-expressing McdA, we set out to reprogram their distribution in *E. coli*, starting with encapsulins.

While bacterial microcompartments (BMCs) like the carboxysome are large complex structures, encapsulins are much smaller (20-45 nm) and simpler protein-based nanocompartments found in bacteria and archaea (*14*). The shell is composed of one or two self-assembling proteins that tiles around an enzymatic cargo loaded via an encapsulin-specific targeting peptide (TP). Like BMCs, encapsulins compartmentalize reaction pathways to sequester toxic intermediates, store reaction products, and increase pathway efficiency, thus offering strategies for specialized metabolic engineering of microbes. No native positioning system has been identified for encapsulins so far.

The study, design, and application of encapsulins rely on their robust expression and assembly in heterologous hosts like *E. coli*. Previous studies have revealed that encapsulins aggregate when expressed in *E. coli* (*2*). Therefore, these encapsulins are ideal substrates for testing the MapTag. Nevertheless, encapsulins have never been visualized in live cells. To address this gap, we first developed a method for live-cell visualization. We engineered an inducible plasmid that expressed an encapsulin shell protein fused to the MapTag, along with a fluorescent cargo protein - mNG fused to a TP (Supplementary Fig. 2A). A degron tag (DT) (*15*) was also fused to mNG to promote degradation of any unencapsulated mNG, thereby enhancing the visualization of mNG-filled encapsulins (*15*). Without McdA, the MapTagged encapsulin foci were nucleoid-excluded to one or both cell poles (Fig. 2A, C-D; Supplementary Fig. 2B-C), consistent with previous work (*2*). But when co-expressed with McdA, several encapsulin foci were distributed along the nucleoid (Fig. 2B-D; Supplementary Fig. B-C).

Having shown that the MapTag can disaggregate and distribute encapsulins in *E. coli*, we next visualized this process in real time. MapTagged encapsulins remained clustered at a single cell pole during the outgrowth of cells lacking McdA (Fig. 2E-F; Video S3). Upon McdA co-expression, encapsulins rapidly redistributed into multiple foci across the cell during outgrowth (Fig. 2G-H; Video S3). Reducing McdA levels caused distributed encapsulins to revert to polar clusters, confirming that positioning requires sustained McdA activity (Fig. 2I-J; Video S4). Conversely, adding McdA to cells with pre-aggregated encapsulins triggered their redistribution along the cell length (Fig. 2K-L; Video S4). Together, these results establish that McdA can spatially control MapTagged encapsulins, with its presence or absence dynamically switching organelles between dispersed and clustered states.

We further performed cryo-ET analysis to confirm that without McdA, the punctate foci represent fully assembled encapsulin clusters confined to the cell pole (Fig. 2M). By contrast, in McdA-expressing cells, encapsulins were no longer restricted to the poles. Instead, we observed encapsulins distributed along the nucleoid region of the cell (Fig. 2N), consistent with fluorescence imaging.

The results thus far demonstrate that the McdAB system from *H. neapolitanus* can be harnessed for minimal, autonomous spatial control of carboxysomes and encapsulins in *E. coli*. α-carboxysomes are both structurally and phylogenetically distinct from β-carboxysomes found in β-cyanobacteria. To extend the versatility of this system, we developed a complementary β-MapTag derived from the N-terminal region of McdB from the β-carboxysome positioning system of the β-cyanobacterium *Synechococcus elongatus*. Expressing β-MapTagged-encapsulins alongside *S. elongatus* McdA, also resulted in encapsulins being distributed across the *E. coli* nucleoid (Supplementary Fig. 2D-H). Together, these findings establish α- and β-MapTags as broadly applicable systems for programmable spatial control of engineered encapsulin nanocompartments.

Spatial control of biomolecular condensates

While BMCs and encapsulins have long been recognized as bacterial organelles, biomolecular condensates have only recently emerged as a distinct strategy for organizing cellular reactions in bacteria (*16*). Their dynamic and reversible nature makes condensates attractive for biotechnology (*17*), yet in bacteria, they typically coalesce into a single polar focus, causing asymmetric inheritance during division (*3*, *18*). To address this limitation, we engineered a condensate positioning system using the MapTag.

S. elongatus McdB forms nucleoid-excluded condensates when expressed in *E. coli* (*18*). We first asked whether McdA could redistribute these condensates on the nucleoid. When expressed alone, mNG-McdA colocalized with the *E. coli* nucleoid (Supplementary Fig. 3A-B). Intriguingly, co-expression with McdB abolished this association. Because McdB condensates are highly fluid-like and a substantial fraction remains cytoplasmic (*18*), we hypothesized that this cytoplasmic McdB pool globally stimulates McdA release from the nucleoid. To reduce these spurious interactions away from the condensate cargo, we fused McdB to the PopTag (*19*), which enhanced McdB sequestration into condensates (Supplementary Fig. 3C-D). Without McdA, McdB^{PopTag} formed one or two large polar condensates (Fig. 3A, C-D). But upon McdA co-expression, multiple condensates were distributed along the nucleoid (Fig. 3B, C-D).

Without McdA positioning, polar condensates were rapidly lost from the cell population (Fig. 3E-F; Video S5). By contrast, in the presence of McdA, all daughter cells inherited roughly an equal complement of McdB^{PopTag} condensates distributed over the nucleoid (Fig. 3G-H; Video S5). Reducing McdA levels resulted in distributed condensates merging back into a single large nucleoid-excluded condensate at the cell pole (Fig. 3I-J; Video S6). Conversely, we observed that replenishing McdA led to the dissolution of polar condensates and the formation of multiple condensates distributed along the nucleoid (Fig. 3K, L; Video S6). Finally, we also confirmed the relocalization of polar condensates to the nucleoid in the presence of McdA by *in situ* cryo-ET (Fig. 3M-N). Our cryo-ET analysis revealed that the addition of tags and the repositioning system does not change the material properties of the condensate.

After successfully engineering a system that allowed us to distribute full-length β-McdB condensates, we set out to identify the minimal β-MapTag sequence for spatially regulating condensates with McdA. The first 20 N-terminal amino acids of β-McdB fused to mCherry^{PopTag} did not yield any condensates (Supplementary Fig. 4A-B). However, addition of the adjacent coiled-coil dimerization domain of β-McdB provided additional valency that restored condensate assembly (Supplementary Fig. 4C). Co-expression of McdA distributed these β-MapTagged condensates along the nucleoid (Supplementary Fig. 4D-F). When swapping the β-MapTag with the α-MapTag, co-expression with its cognate McdA resulted in condensate dissolution over the nucleoid (Supplementary Fig.

4G-I), suggesting the α-MapTag may be more suitable for positioning condensates with lower saturation concentrations. Together, we demonstrate that McdA can direct the spatial organization of both McdB condensates and MapTagged condensates, ensuring their cellular distribution and faithful inheritance across the cell population.

Spatial control of a membrane-bound organelle

To test the versatility and robustness of MapTags, we determined if this mode of spatial control could be extended beyond protein-based compartments to include membrane-bound organelles. Ferrosomes are membrane-bound compartments for iron storage that require the membrane protein FezA and the P1B6-ATPase transporter FezB for their formation (*20*). Heterologous expression of FezA and FezB in *E. coli* induces the formation of these lipid-bound compartments. Expression of mNG-FezB fused to the α-MapTag, along with untagged FezA, resulted in the formation of ferrosome clusters at the cell pole (Fig. 4A, C-D; Supplementary Fig. 5A-B). Upon co-expression of McdA, multiple ferrosome foci were observed over the nucleoid (Fig. 4B, C-D; Supplementary Fig. 5A-B). A co-expression time course showed McdA ensuring the cellular distribution and faithful inheritance of assembling ferrosomes across the cell population (Fig. 4E-F). We observed that McdA was also able to partition preformed ferrosome clusters at the cell pole and redistribute them over the nucleoid (Fig. 4G-H). Finally, we observed that using the β-MapTag to FezB was just as effective in distributing ferrosomes as the α-MapTag (Supplementary Fig. 5C-D).

Discussion

We establish spatial control as a new design principle in bacterial synthetic biology. By reconstituting and repurposing McdAB, we show that a minimal, two-protein positioning module can be harnessed to restore the native organization of carboxysomes and, more broadly, to spatially reprogram the distribution of diverse bacterial organelles in *E. coli*. The capacity to engineer both the composition of cellular compartments and their precise intracellular positioning advances synthetic biology into a new era, where the spatial context of cellular function (“where”) can be programmed as readily as its molecular content (“what”).

The impact of this spatial control extends beyond simple organelle placement. We demonstrate that mislocalized carboxysomes in *E. coli* also suffer structural defects. McdAB corrects this by transforming disordered polar aggregates into properly sized and structurally intact organelles distributed over the nucleoid, restoring both assembly fidelity and inheritance. By generalizing this approach with MapTags, we extend spatial control to encapsulins, condensates, and ferrosomes - representing the full spectrum of known protein-based and lipid-bound organelle types. These results suggest that spatial

misregulation may be a universal bottleneck for heterologous organelle engineering, and that positioning systems provide a general solution.

This conceptual advance parallels the way cytoskeletal elements and trafficking systems underpin compartmentalization in eukaryotes. Whereas eukaryotes evolved complex, multi-component transport machinery, bacteria have distilled spatial organization into minimal ATP-driven modules that establish self-organizing gradients. By reengineering this strategy, we unlock a scalable, orthogonal method for positioning organelles in bacterial cells. The versatility of α- and β-MapTags across structurally distinct compartments underscores their potential as modular “address labels” for intracellular engineering.

Programmable organelle positioning opens several future directions. First, it enables the rational design of metabolic “reaction landscapes” in bacteria, where organelles can be spaced to prevent interference, aligned to channel substrates, or dynamically repositioned in response to environmental signals. Second, because McdAB activity is reversible, spatial organization can be toggled on or off, allowing for time-dependent control of metabolism or stress responses. Third, distributing compartments evenly across the nucleoid ensures faithful inheritance, reducing population-level heterogeneity and thereby improving the reliability of engineered microbial systems. By layering spatial control onto existing advances in compartment design, we foresee the emergence of “organelle engineering” as a discipline in its own right - where the content, function, and location of organelles can all be rationally specified. Such a framework could accelerate the development of microbial cell factories for carbon capture, green chemistry, and therapeutics.

Beyond biotechnology, this work provides a blueprint for constructing synthetic cells. A central question in bottom-up biology is how to couple self-assembly with inheritance. Our results demonstrate that a minimal gradient-based system is sufficient to transform self-assembling but static compartments into dynamic, heritable organelles.

Acknowledgements

We thank Dr. Eric Rentchler and Dr. Sasha Meshinchi of the Biomedical Microscopy Core at the University of Michigan for training and coordinating access to the super-resolution Airyscan Microscope. A provisional patent application related to this work (PCT/US24/50743) has been filed.

Funding:

National Science Foundation grant 1941966 (A.G.V)

National Institutes of Health grant R35GM152128 (A.G.V.)

National Institutes of Health 1K99GM157383-01 (Y.H.)

National Institutes of Health 1DP2GM150019-01 (S.M.)

Klatskin Sutker Discovery Fund (S.M.)

National Institutes of Health grant S10OD030275 (S.M.)

Arnold and Mabel Beckman Foundation award to the University of Michigan Cryo-EM facility

National Institutes of Health grant R35GM133325 (T.W.G.)

National Science Foundation grant 2342136 (T.W.G.)

National Institutes of Health T32 GM145304 (J.A.B.)

Rackham Predoctoral Fellowship and Asan Foundation Biomedical Science Scholarship (S.K.)

The funders had no role in the study design, data collection, analysis, or the content and publication of this manuscript.

Author contributions:

Conceptualization: A.G.V. and Y.H.

Methodology: A.G.V., Y.H., P.V.J., D.S.T., R.E.D., S.K., K.T., J.A.B., C.A.A., T.W.G., H.P., and S.M.

Investigation: A.G.V., Y.H., P.V.J., S.M.

Visualization: A.G.V., Y.H., R.E.D., J.A.B.

Funding acquisition: A.G.V., Y.H., S.M., T.W.S., H.P.

Project administration: A.G.V. and Y.H.

Supervision: A.G.V. and S.M.

Writing – original draft: A.G.V. and Y.H.

Writing – review & editing: All authors

Competing interests:

The authors declare that they have no competing interests.

Data and materials availability

All plasmids are available at Addgene. Data processing and analysis scripts for this study are available on GitHub.

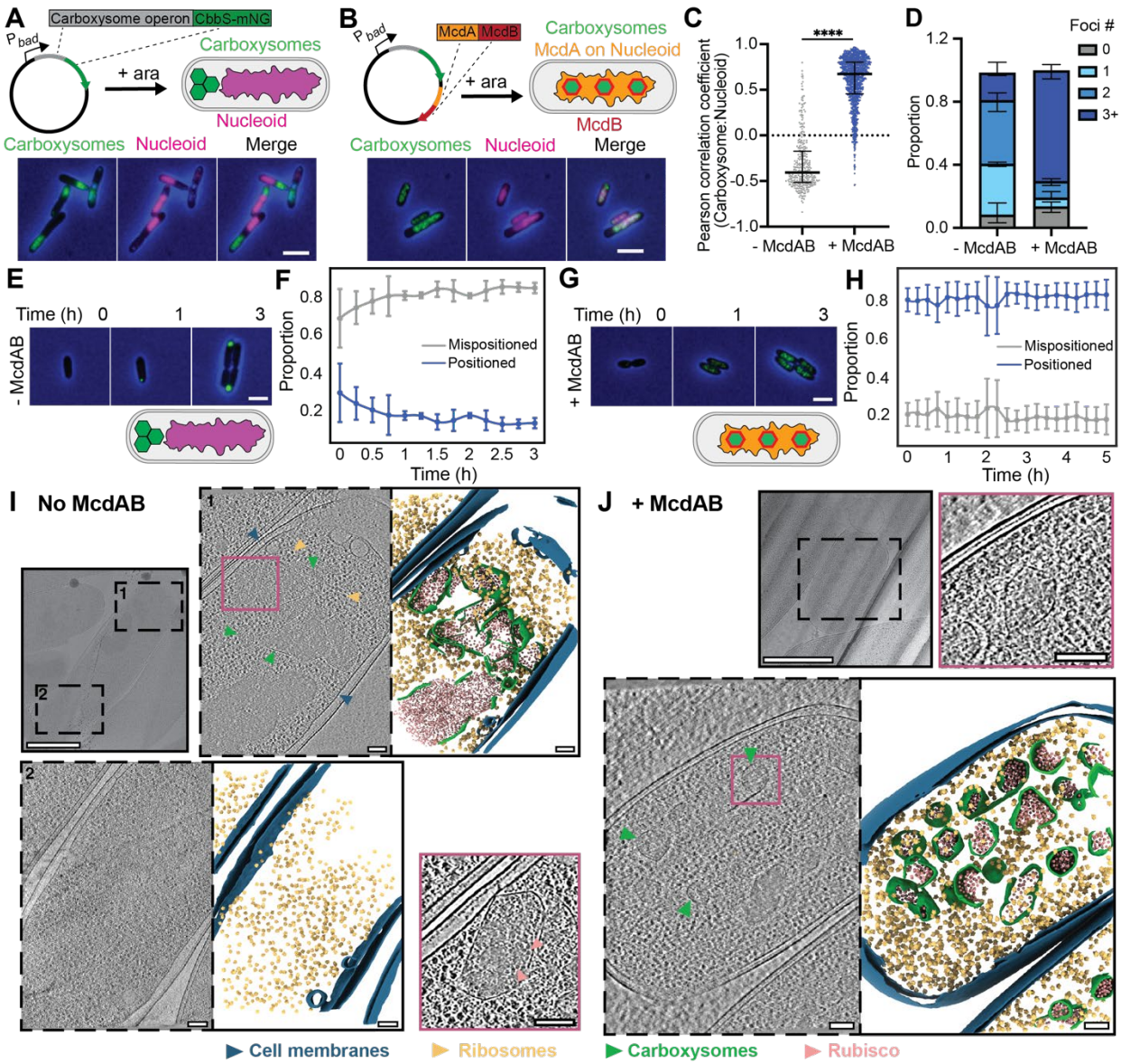

Figure 1. The McdAB system spatially organizes carboxysomes on the *E. coli* nucleoid. (**A**, **B**) Schematic and wide-field fluorescence images of *E. coli* cells expressing carboxysomes without (A) or with (B) the McdAB system. The small subunit of Rubisco (CbbS) is fused to mNeonGreen (mNG); protein expression is induced with 0.2% arabinose (ara). Unless specified, mNG-labeled carboxysomes are shown in green, DAPI-stained nucleoids in magenta, and phase-contrast in blue; scale bar, 2 µm. (**C**) Pearson correlation coefficients measuring colocalization between mNG-carboxysomes and DAPI-stained nucleoids. (**D**) Quantification of the proportion of cells with indicated numbers of carboxysome foci. (**E**–**H**) Time-lapse analysis showing images and quantification of carboxysome positioning over time with (E, F) or without (G, H) McdAB. Proportions of cells with mispositioned (0–2 polar foci) and positioned (≥ 3 distributed foci) carboxysomes are plotted over time. (**I, J**) Cryo-electron tomography of *E. coli* without (I) or with (J) the McdAB system. In each case, low-magnification (6500×) transmission electron microscopy (TEM) images are shown to the left and indicate sites of tomography tilt

series data acquisition (dashed boxes). Representative slices through tomograms (dashed boxes) and corresponding segmentations of the tomograms are shown in each case. Cellular features are highlighted as carboxysomes (green), Rubisco (pink), ribosomes (orange), and cell membranes (blue). Zoomed-in views (pink boxes) provide higher-magnification images of carboxysomes (with Rubsico marked with pink arrowheads). Scale bars: 500 nm (overview), 100 nm (zoom-in).

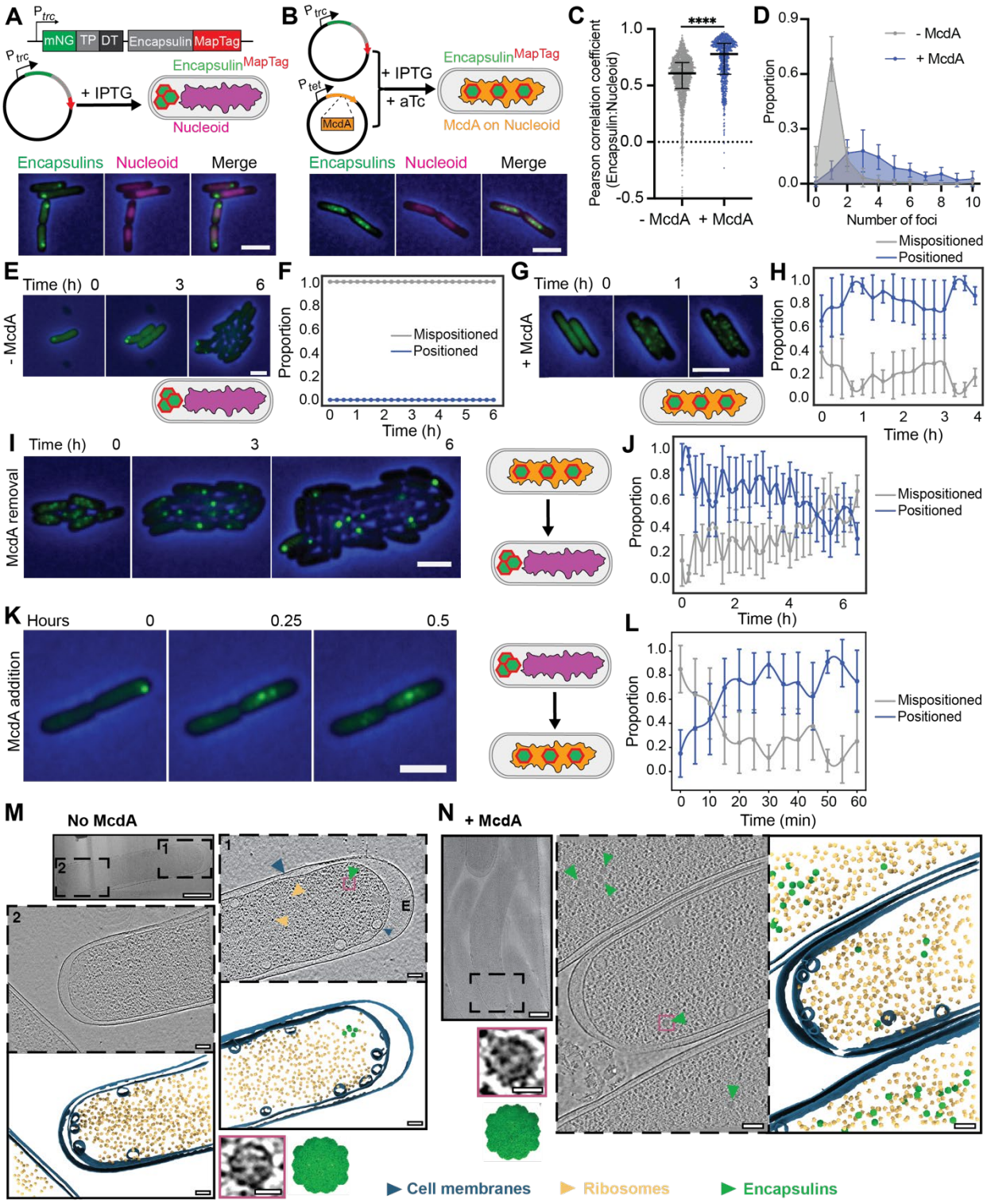

Figure 2. McdA distributes MapTagged encapsulins on the *E. coli* nucleoid. (**A**) Schematic and wide-field fluorescence images of *E. coli* cells expressing encapsulins fused to the MapTag and mNeonGreen (mNG) cargo fused to an encapsulin-specific targeting peptide (TP) and a degron tag (DT), under the P_{trc} promoter with IPTG induction. (**B**) As in (A), but with McdA co-expressed from a separate plasmid under the P_{tet} promoter, induced with anhydrotetracycline

(aTc). Unless specified, mNG-labeled encapsulins are shown in green, DAPI-stained nucleoids in magenta, and phase-contrast in blue; scale bars, 2 µm. (**C**) Pearson correlation coefficients measuring colocalization between mNG-encapsulins and DAPI-stained nucleoids. (**D**) Quantification of the proportion of cells with the indicated number of encapsulin foci. (**E**–**H**) Time-lapse analysis showing images and quantification of encapsulin positioning over time in cells without (E, F) or with (G, H) McdA; proportions of cells with mispositioned (0–2 polar foci) and positioned (≥3 distributed foci) encapsulins are shown. (**I**–**L**) Reversible control of encapsulin positioning through McdA removal (I, J) or addition (K, L), as shown by images and quantification of positioned and mispositioned encapsulins over time. (**M**, **N**) Cryo-electron tomography of encapsulin^{MapTag}-containing *E. coli* without (M) or with (N) McdA. In each case, low-magnification (6500×) transmission electron microscopy (TEM) images are shown to the left and indicate sites of tomography tilt series data acquisition (dashed boxes). Representative slices through tomograms (dashed boxes) and corresponding segmentations of the tomograms are shown in each case. Cellular features are highlighted as encapsulins (green), ribosomes (orange), and cell membranes (blue). Zoomed-in views (pink boxes) provide higher-magnification images of fully assembled encapsulins. Scale bars: 500 nm (overview), 100 nm (zoom-in).

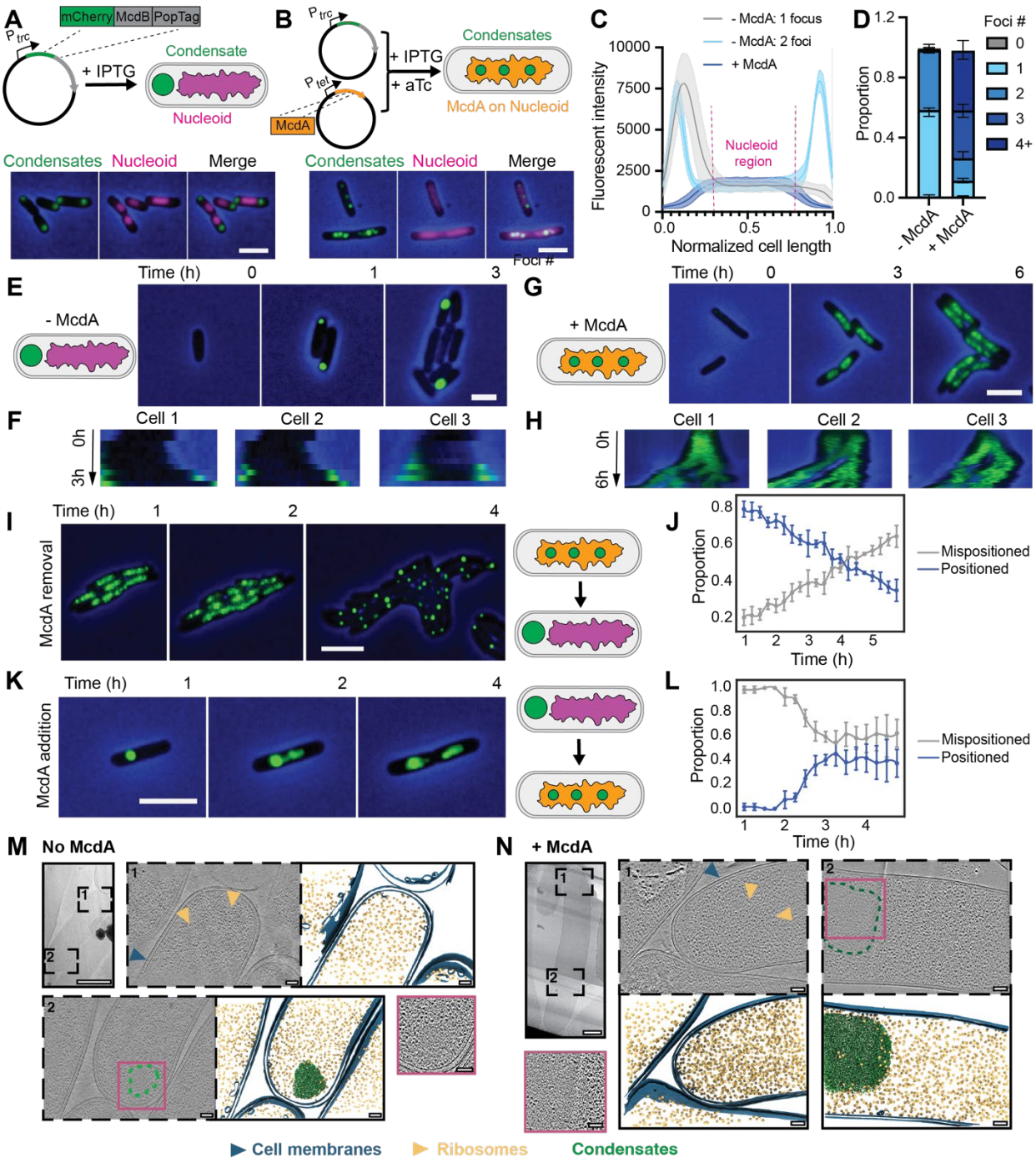

Figure 3. McdA distributes McdB condensates on the *E. coli* nucleoid. (**A**) Schematic and wide-field fluorescence images of *E. coli* cells expressing McdB condensates fused to mCherry and PopTag, under the P_{trc} promoter with IPTG induction. (**B**) As in (A), but with McdA co-
5 expressed from a separate plasmid under the P_{tet} promoter, induced with anhydrotetracycline (aTc). Unless specified, $McdB^{PopTag}$ condensates are shown in green, DAPI-stained nucleoids in magenta, and phase-contrast in blue; scale bars, 2 µm. (**C**) Fluorescent intensity profiles of $McdB^{PopTag}$ signal along the normalized cell length. (**D**) Quantification of the proportion of cells with the indicated number of $McdB^{PopTag}$ condensates. (**E–H**) Time-lapse analysis showing wide-

field fluorescence images (E, G) and kymographs of representative cells (F, H) depicting the distribution of McdB^{PopTag} fluorescence over time without (E, F) or with (G, H) of McdA. (**I–L**) Reversible control of McdB^{PopTag} condensate positioning by McdA removal (I, J) or addition (K, L), shown by wide-field fluorescence images and quantification of positioned(≥3 distributed foci) and mispositioned (0–2 polar foci) condensates over time. (**M**, **N**) Cryo-electron tomography of *E. coli* expressing McdB^{PopTag} condensates without (M) or with (N) McdA. In each case, low-magnification (6500×) transmission electron microscopy (TEM) images are shown to the left and indicate sites of tomography tilt series data acquisition (dashed boxes). Representative slices through tomograms (dashed boxes) and corresponding segmentations of the tomograms are shown in each case. Cellular features are highlighted as condensates (green), ribosomes (orange), and cell membranes (blue). Zoomed-in views (pink boxes) provide higher-magnification images of condensates seen as ribosome-excluded areas. Scale bars: 500 nm (overview), 100 nm (zoom-in).

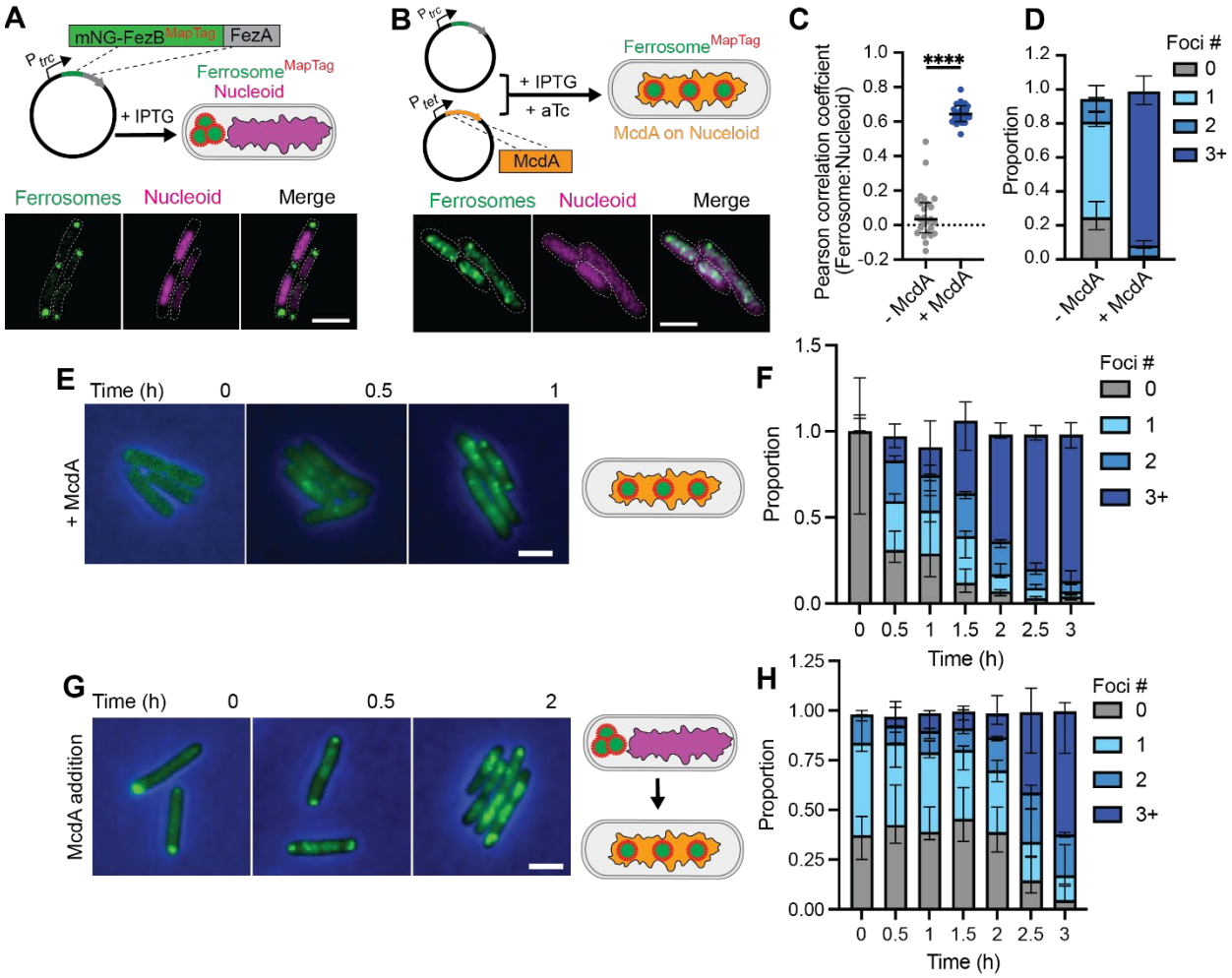

Figure 4. McdA distributes MapTagged ferrosomes on the *E. coli* nucleoid. (**A**) Schematic and super-resolution Airyscan images of *E. coli* cells expressing ferrosomes, composed of FezA and FezB (with FezB fused to mNeonGreen [mNG]), under the P_{trc} promoter with IPTG induction. (**B**) As in (A), but with McdA co-expressed from a separate plasmid under the P_{tet} promoter, induced with anhydrotetracycline (aTc). Unless specified, ferrosomes are shown in green, DAPI-stained nucleoids in magenta, and phase-contrast in blue. Scale bars, 2 µm. (**C**) Pearson correlation coefficients measuring colocalization between mNG-labeled ferrosomes and DAPI-stained nucleoids. (**D**) Quantification of the proportion of cells with the indicated number of ferrosome foci. (**E**, **F**) Wide-field fluorescence images (E) and quantification (F) of ferrosome positioning over time in cells with McdA over time. (**G**, **H**) Wide-field fluorescence images (G) and quantification (H) showing the redistribution of ferrosomes upon McdA addition to cells initially lacking McdA over time.